Journal of Achievements in Materials and Manufacturing Engineering
VOLUME 48
ISSUE 1
September
2011

Selected mechanical properties and microstructure of Al_2O_3-ZrO_{2nano} ceramic composites

M. Szutkowska [a,b,*], B. Smuk [b], A. Kalinka [b], K. Czechowski [b], M. Bućko [c], M. Boniecki [d]

[a] Institute of Technology, Pedagogical University, ul. Podchorążych 2, 30-084 Kraków, Poland

[b] Centre of Materials Engineering and Sintering Techniques, Institute of Advanced Manufacturing Technology, ul. Wrocławska 37a, 30-011 Kraków, Poland

[c] Department of Materials Engineering and Ceramics, University of Science and Technology, Al. Mickiewicza 30, 30-059 Kraków, Poland

[d] Department of Ceramics, Institute of Electronic Materials Technology, ul. Wólczyńska 133, 01-919 Warszawa, Poland

* Corresponding author: E-mail address: magdaszut@ap.krakow.pl

Received 23.07.2011; published in revised form 01.09.2011

Properties

ABSTRACT

Purpose: Basic mechanical properties of the studied tool materials and microstructure of alumina-zirconia ceramic composites with fraction of nanopowders have been presented.

Design/methodology/approach: The present study reports selected properties obtained by reinforcing Al_2O_3 with 15 wt% ZrO_2 (partially stabilized with Y_2O_3-Y5) and, non-stabilized zirconia. Specimens were prepared based on submicro- and nano-scale trade powders. Vickers hardness (HV1), wear resistance and fracture toughness (K_{IC}) at room and elevated temperatures characteristic for tool work were evaluated. Microstructure was observed by means of a scanning electron microscopy (SEM). Preliminary industrial cutting tests in the turning of higher-quality carbon steel C45 grade were carried out.

Findings: The addition of nanopowders does not result in a significant improvement in fracture toughness at room temperature. A reduction in fracture toughness of $K_{IC(ET)}$ by approximately 20% is observed at elevated temperature (1073 K) for the specimen only with submicro powders in comparison to that at room temperature. Addition of the powder mixture in submicron and nano scale size reveals the minor reduction of fracture toughness (up to 10%) at elevated temperature.

Practical implications: The results show that using of powders in submicron and nano scale size not improve the tool life but influences the fracture toughness et elevated temperatures.

Originality/value: The results of the presented investigations allow rational use of existing ceramic tools.

Keywords: Al_2O_3-ZrO_{2nano} ceramics; Indentation fracture toughness; Vickers hardness; SEM image

Reference to this paper should be given in the following way:
M. Szutkowska, B. Smuk, A. Kalinka, K. Czechowski, M. Bućko, M. Boniecki, Selected mechanical properties and microstructure of Al_2O_3-ZrO_{2nano} ceramic composites, Journal of Achievements in Materials and Manufacturing Engineering 48/1 (2011) 58-63.

1. Introduction

Regardless the brittle nature of structural ceramics, this class of materials revels interesting properties for high-speed cutting tools. In addition to inherent high hot-hardness, ceramics also resist high temperatures without deforming, exceeding the capabilities of cemented carbides (WC-Co). This allows tools to cut at faster speeds and deeper depths, resulting in increased removal rates and, consequently, cost efficient machining [1]. Oxide ceramic materials feature high melting temperature, relatively low density and low thermal conductivity as well as considerable corrosion resistance to chemical active media in high temperatures [2, 3, 4]. Addition of zirconia to alumina allows to receive zirconia-toughened alumina (ZTA) ceramics, in which the strength and toughness have been improved due to stress induced t-m transformation. In particular, thanks to its good mechanical properties, zirconia-toughened alumina (ZTA) has widened the scope of application of oxide ceramics and is effectively used in the manufacture of cutting tools, dies or prosthetic components [5, 6]. Rapid developments in the micro-structure of basic ceramics have introduced ceramic-ceramic composites for many engineering applications. It is generally known that Al_2O_3–ZrO_2 composites and nanocomposites have better mechanical properties than Al_2O_3 and ZrO_2 because of the dispersion of metastable tetragonal zirconia particles in the alumina matrix, which transform into the stable monoclinic phase under loading. The properties of these materials are determined by their microstructures; therefore, to control their microstructural development and achieve fine microstructures, the sintering parameters must be optimized. The synthesis of nanomaterials in powder form has been successfully demonstrated in a large number of materials; however, the synthesis of nanostructured materials in bulk form remains largely unachieved. The sintering of nanopowders to full or nearly full density without appreciable grain growth continues to present a significant practical challenge [7]. The production of fully dense ceramic materials with nanosize features has received an increasing attention over the recent years in view of several industrial applications, because of the expected or even already achieved improvements in mechanical and/or functional performances. However, a successful approach to nanostructuration requires the development of innovative concepts to be applied in each step of the ceramic manufacturing chain, starting from the tailoring of a suitable raw material, the ceramic powder [8]. On the other hand, the use of metastable zirconia particles as a reinforcing element improves the wear resistance through the suppression of crack initiation and propagation due to the higher value of the fracture toughness. The transformed particles in the near-surface area induce a compressive stress field, which serves as a toughening mechanism: it reduces the crack-driving force for any existing surface or subsurface cracks (Fig. 1) [9, 10]. The micro/nano-composite with inter/intragranular ZrO_2 nanoparticles provides the possibility to design new materials with toughening mechanisms operating on a scale smaller than that of the matrix microstructure. This enhances the ''intrinsic'' fracture properties of these materials and their wear resistance in the mild regime [9].

The enhancement in toughness is limited by the coarsening effect of ZrO_2 particles during sintering of the composites. A smaller initial particle size and a uniform distribution of fine

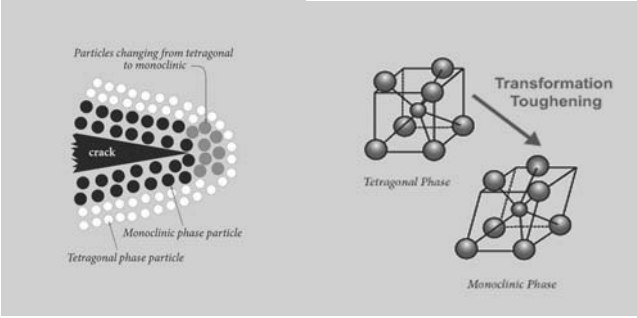

Fig. 1. Transformation toughening mechanism scheme at the crack tip of zirconia [9]

ZrO_2 particles in tetragonal form is the desirable microstructure for toughened Al_2O_3-ZrO_2 composites. A finer particle size distribution of ZrO_2 not only helps to achieve a uniform distribution of ZrO_2 particles, but it also ensures that ZrO_2 remains mostly in tetragonal phase provided the critical size barrier for the t-phase retention is not crossed [11]. Higher volume fraction of ZrO_2 is expected to increase the fracture toughness of the composites due to higher volume fraction of tetragonal ZrO_2 available for stress induced transformation. The presence of relatively large monoclinic zirconia particles at grain boundaries creates sufficient stresses to cause microcracking at the alumina-zirconia interfaces, that in some cases, extends along the alumina-alumina grain boundaries [12]. The extent of toughening achieved in this composite depend on the particle size of Al_2O_3 and ZrO_2 , volume fraction of ZrO_2 retained in the metastable tetragonal phase as well as on the relative distribution of Al_2O_3 and ZrO_2 in the matrix [13]. A major problem in achieving a high density Al_2O_3-ZrO_2 composites is the coarsening of ZrO_2 particles during high temperature processing. The coarsening of ZrO_2 will not only adversely affect the densification behaviour but also will reduce the retained tetragonal ZrO_2. Thus efforts are being made to prepare ultrafine particles of Al_2O_3 and ZrO_2 through different improved processing routes. The specific advantages of these ultrafine powders are superior phase homogeneity and low temperature sinterability. A uniform powder shape having a continuous and narrow size distribution are expected to yield products with reduced microstructural defects due to improved powder flowability and better packing density [14]. Variation of the sintering conditions leads to nanocomposites with different microstructural features, such as grain sizes and inter- or intragranular location of zirconia reinforcement [15]. Fully-dense ceramics with grain size approaching 10 nm could be routinely obtained using a high-pressure modification of the field activated sintering (spark plasma sintering). Using the high pressure up to 1 GPa, high heating rates and short sintering time sintering temperature can be much lower than the temperatures used in conventional sintering methods [16]. In this paper, we report the effect of reduction powder size from submicron scale to nano scale of phase components in alumina-zirconia ceramic composites on micro-structure and selected mechanical properties. The main goal of this investigation is to enhance possibility of using this materials as a cutting tools.

2. Experimental procedure

Alumina, zirconia partially stabilized with yttria, non-stabilized zirconia were used as raw materials to manufacture the alumina-15 wt% zirconia composites. A commercial Alcoa alumina powder (containing 85.0 % α-phase, of 99.8% purity) type A16SG with a submicron particle size of below 0.5 μm and a nano particle size of 40 nm, with average size of agglomerates of 150 nm produced by Inframat Advanced Materials, USA were used to prepare the tested composites. Experiments were carried out on alumina-based composites with the addition of: 10 wt% ZrO_2 with modification of the zirconia phase (partially stabilized with 5 wt% Y_2O_3–PYT05.0 (ZY5) produced by Unitec Ceramics, England, with an average particle size of 0.9-1.1 μm; ZrO_2 stabilized with 3% mol. Y_2O_3 produced by Inframat Advanced Materials, USA (marked as YSZ_{nano}) and a monoclinic phase of zirconia in submicron (m-ZrO_2) and nano (30-60 nm) scale (m-ZrO_{2nano}) produced by Fluka, Germany. Sintering additives, such as MgO_{nano} (0.3 wt%), were introduced to inhibit grain growth. The initial compositions of compounds selected for testing are presented in Table 1.

Table 1.
Composition of selected compounds

Compound	Compound composition, wt%					
	Al_2O_3		ZY5		m-ZrO_2	
	μm	nm	μm	nm	μm	nm
A	85.0	—	9.0	—	6.0	—
A1	42.5	42.5	4.5	4.5	3.0	3.0

Components were mixed for approximately thirty hours in alumina mills with zirconia balls, with the addition of a plasticizer. Materials, uniformly set, after plasticizing and drying, were granulated. Green compacts with dimensions of 5.5 ×3.0 ×35 mm and 16.5x16.5x10 mm were uniaxially pressed at 100 MPa and then cold isostatically pressed at 200 MPa. Ceramic composites were sintered at a maximum temperature of 1923 K at constant heating and cooling rates of the furnace.

Following measurements were performed on the tested specimens: Vickers hardness HV1, fracture toughness at room temperature K_{IC}, fracture toughness at an elevated temperature of 1073 K $K_{IC(ET)}$, wear resistance v_n (determined by speed of mass loss), apparent density ρ_p, and porosity P_c (determined by the hydrostatic method). Single Edge Notched Beam (SENB) specimens (mechanically notched) with dimensions 1.5×4.0×35.0±0.1 mm were used to determine fracture toughness by means of a conventional method based on three-point bending of specimens (3PB) [17, 18]. An initial 0.9 mm deep notch was produced a diamond saw (thickness 0.20 mm) and then the notch tip was pre-cracked with a thin diamond saw (thickness 0.025 mm). The total initial notch length was approximately 1.1 mm. The relationship $K_{IC} = f(c)$ is given by the equations (1,2) [19]:

$$K_{IC} = 1.5\frac{P_c S}{W^2 B} Yc^{1/2} \tag{1}$$

$$Y = \frac{\sqrt{\Pi}}{(1-\beta)^{\frac{3}{2}}}\left[0.3738\beta + (1-\beta)\sum_{i,j=0}^{4} A_{ij}\beta^i\left(\frac{W}{S}\right)^j\right] \tag{2}$$

where: P_c – critical load, S – support span, W – width, B – specimen thickness, Y – a geometric function, c – crack length, β – c/W and A_{ij} is the coefficients given by Fett [17].

Measurements of critical intensity factor an elevated temperature of 1073 K were carried out on a ZWICK 1446 instrument with mounted electrical furnace (Fig. 2).

Fig. 2. Measuring position for determination of fracture toughness at elevated temperatures

Modulus of elasticity (Young's modulus) of the tested composites was determined by a measuring the transmission velocity of longitudinal and transversal ultrasonic waves through the sample using ultrasonic flaw detector Panametrics Epoch III. The accuracy of calculated Young's modulus estimated at 2 %. Calculations were made using the following formula:

$$E = \rho C_T^2 \frac{3C_L^2 - 4C_T^2}{C_L^2 - C_T^2} \tag{3}$$

where: E – Young's modulus, C_L – velocity of the longitudinal wave, C_T – velocity of the transversal wave, ρ – density of the material.

The velocities of transversal and longitudinal waves were determined as a ratio of sample thickness and relevant transition time. The accuracy of calculated Young's modulus from equation (3) was estimated to be below 2 %.

Wear resistance was determined by a method based on the measurement of mass decrement rate during wear of the specimen against an SiC80 abrasive cloth. The following formula was used to calculate mass decrement rate (Vn):

$$V\text{n} = \frac{1000 \cdot \Delta m}{\rho_P \cdot F \cdot T} \quad [\mu\text{m/h}] \tag{4}$$

where: Δm – absolute mass wear, ρ_p – apparent density, F – specimen contact surface, T – time.

Microstructure observations of the specimen were carried out using a JEOL JSM-6460LV scanning electron microscope. X-ray diffraction was used both to identify phases and to assess the percentage fraction of tetragonal zirconia phase (t) and monoclinic zirconia phase (m). Preliminary cutting tests in the turning of higher-quality carbon steel C45 grade with hardness in the range 167-179 HB were carried out for CSRNL2525-12 type inserts. Tool life (T_{mean}) of the insert cutting edge was measured for tested composite inserts at the following cutting parameters: speed (v_c) = 220 m/min, feed (f) = 0.15 mm/rev., depth (a_p) = 1.0 mm, wear criterion (higher values of wear on flank face from measured VB_{Bmax} and VB_C values were accepted) VB = 0.30 mm (Fig. 3)

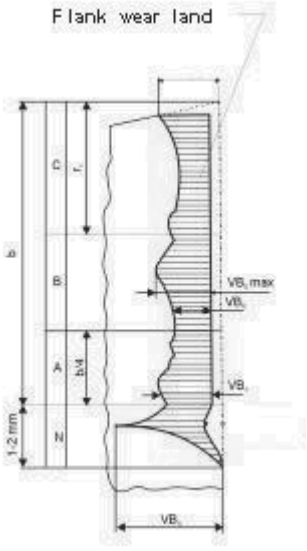

Fig. 3. Flank wear land with different type of cutting edge wear

Cutting tests were performed without cooling lubricant.

3. Results and discussion

The results obtained from the tests concerning: apparent density ρ_p, and total porosity P_c of tested alumina-zirconia ceramic composites with various compositions (A, A1) are presented in Table 2. Tested alumina-zirconia composites exhibit: high Vickers hardness HV1 (in the range 18.1-18.2 GPa), similar values of elastic modulus (348-375 GPa) and a lower mass decrement ratev_n10^3 (5.0-5.3 μm/h) in relation to pure alumina.

The results obtained from mechanical tests are shown in Table 3.

Table 2.
Selected physical properties of tested ceramic composites: apparent density ρ_p, porosity P_c

Material	Apparent density ρ_p [g/cm^3]	Porosity P_c [%]
A	4.14	1.75
A1	4.15	1.50

Table 3.
Selected mechanical properties of tested ceramic composites: Young's modulus E, Vickers hardness HV1, fracture toughness at room temperature K_{IC} and elevated temperature (1073 K) $K_{IC(ET)}$, wear resistance v_n

Material	Vickers hardness HV1 [GPa]	Young's modulus E [GPa]	Critical stress intensity factor K_{IC} [MPa m$^{1/2}$]	Critical stress intensity factor $K_{IC(ET)}$ [MPa m$^{1/2}$]	Wear resistance $v_n 10^3$ [μm/h]
A	18.1	348	4.44	3.57	5.0
A1	18.2	375	4.45	4.07	5.3

Both specimen (A) manufactured only on the submicron powder basis and (A1) with fraction of mixed submicron and nano powder reveal similar values of critical stress intensity factor K_{IC} at room temperature (in the range 4.44-4.45 MPa m$^{1/2}$). A reduction in fracture toughness of $K_{IC(ET)}$ by approximately 20% is observed at elevated temperature (1073 K) for the (A) specimen (only submicro powder) in comparison to that at room temperature. The microstructure of the alumina-zirconia composites surface is presented in Figures 4 and 5.

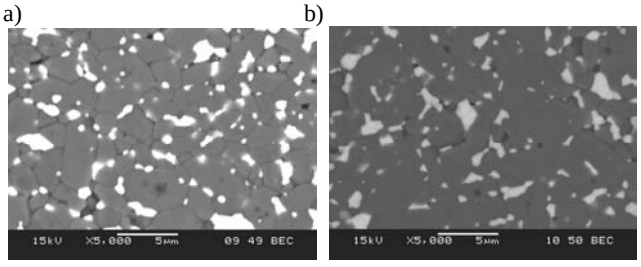

Fig. 4. SEM micrographs of a surface of the Al_2O_3-ZrO_2 ceramic composites at 5000x magnification: a) (A) specimen, b) (A1) specimen (zirconia – grains in white colour)

However, for specimen (A1) with using the mixture submicron and nano scale size of powder reduction of fracture toughness is minor than 10%. X-ray diffraction analysis for the characterization of the ceramic composites were made as a completion study. The Rietvelda method with X'Pert Plus programme was used for quantitative phase analysis of ceramics. The Philips program APD-3.5B-Fit profile was used for observation wt% content of revealed phases. X-ray diffraction analysis of tested ceramic composites is presented in Figs. 6 a, b.

a) b)

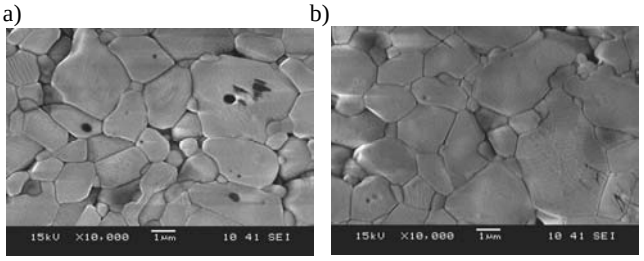

Fig. 5. SEM micrographs of a surface of the Al_2O_3-ZrO_2 ceramic composites at 10000x magnification: a) A specimen, b) A1 specimen

a)

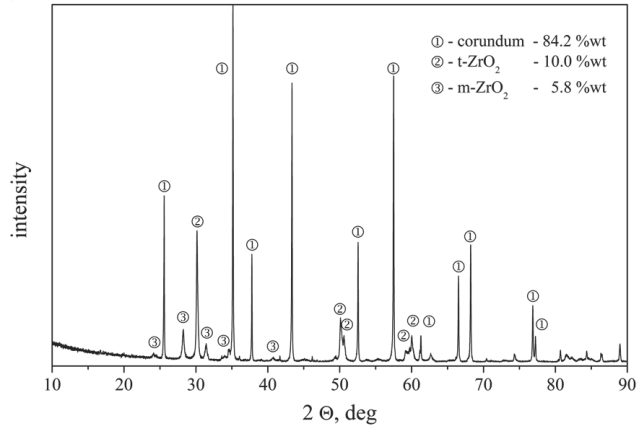

b)

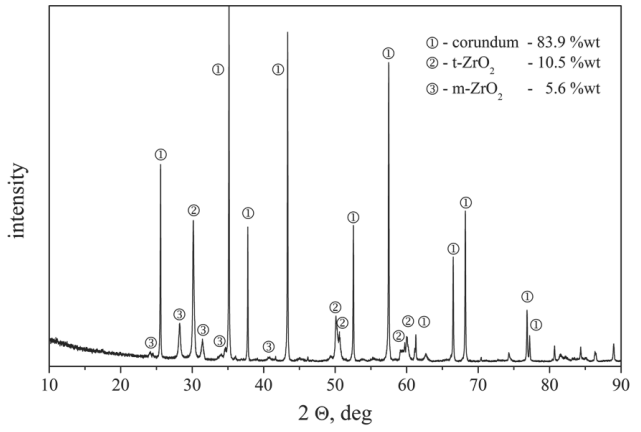

Fig. 6. X-ray diffraction analysis of tested ceramic composites: a) A specimen, b) A1 specimen

This diffraction indicates 84.2 wt% α-Al_2O_3, 5.8 wt% m-ZrO_2 (monoclinic phase) and 10.0 wt% t-ZrO_2 (tetragonal phase) for A specimen. Fraction of elements for A1 sample is in the same range 83.9 wt% α-Al_2O_3, 5.6 wt% m-ZrO_2 (monoclinic phase) and 10.5 wt% t-ZrO_2 (tetragonal phase).

Results of a cutting test carried out on the tested alumina-zirconia ceramic composites reveal a similar tool life for the (A) composite (T_{mean}=32.5 min) and (A1) composite (T_{mean}=30.2 min) at the accepted wear criterion *VB* = 0.30 mm (Fig. 7).

a)

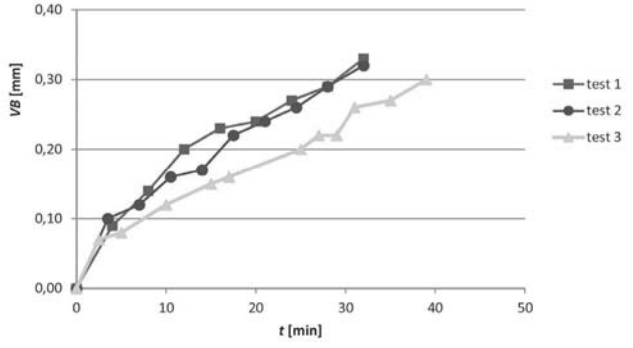

b)

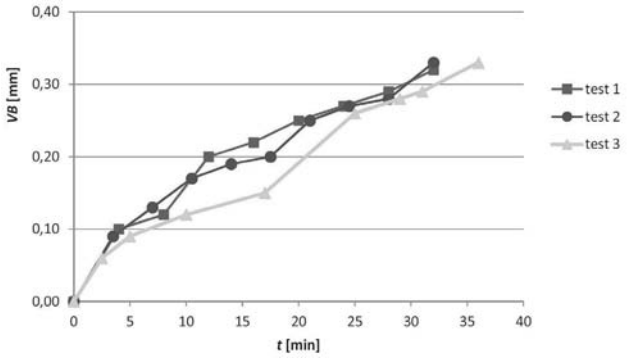

Fig. 7. Results of wear edge measurements at turning of tested ceramic inserts : a) A specimen, b) A1 specimen

4. Conclusions

Alumina-zirconia composites Al_2O_3-15wt% ZrO_2 exhibit: high Vickers hardness HV1 (in the range 18.1-18.2 GPa), similar values of elastic modulus E (348-375 GPa) and a lower mass decrement rate v_n10^3 (5.0-5.3 μm/h) in relation to pure alumina. Both specimen (A) manufactured only on the submicron powder basis and (A1) with fraction of mixed submicron and nano powder reveal similar values of critical stress intensity factor K_{IC} at room temperature (in the range 4.44-4.45 MPa $m^{1/2}$). A reduction in fracture toughness of $K_{IC(ET)}$ by approximately 20% is observed at elevated temperature (1073 K) for the (A) specimen (only submicron powder) in comparison to that at room temperature. However, for specimen (A1) with using the mixture submicron and nano scale size of powder reduction of fracture toughness is minor than 10%. The similar growth of the alumina grains after sintering (average size is 1.6 μm) is observed in both specimens in comparison to initial size of the alumina powder. Size of zirconia grains in monoclinic and tetragonal phase remain at an initial

level (about 40 nm). The results of the presented investigations allow rational use of existing ceramic tools.

References

[1] W. Acchar, A.E. Martinelli, C.A.A. Cairo, Reinforcing Al_2O_3 with W-Ti mixed carbide, Materials Letters 46/4 (2000) 209-211.

[2] K. Kobylańska-Szkaradek, Thermal barrier ZrO_2-Y_2O_3 obtained by plasma spraying method and laser melting, Archives of Materials Science and Engineering 36/1 (2009) 12-19.

[3] P. Putyra, M. Podsiadło, B. Smuk, Alumina-Ti(C,N) ceramics with TiB_2 additives, Archives of Materials Science and Engineering 47/1 (2011) 27-32.

[4] L.A. Dobrzański, M. Kremzer, A. Nagel, B. Huchler, Fabrication of ceramic preforms based on Al_2O_3 CL 2500 powder, Journal of Achievements in Materials and Manufacturing Engineering 18 (2006) 71-74.

[5] S. Biamino, P. Fino, M. Pavese, C. Badini, Alumina-zirconia-yttria nanocomposites prepared by solution combustion synthesis, Ceramics International 32/5 (2006) 509-513.

[6] M. Szutkowska, B. Smuk, M. Boniecki, Titanium carbide reinforced composite tool ceramics based on alumina, Advances in Science and Technology 65 (2010) 50-55.

[7] R.R. Menezes, R.H.G.A. Kiminami, Microwave sintering of alumina-zirconia nanocomposites, Journal of Materials Processing Technology 203 (2008) 513-517.

[8] P. Palmero, V. Naglieri1, M. Azar, V. Garnier, M. Lombardi, L. Joly-Pottuz, J. Chevalier, L. Montanaro, Nanopowder engineering: from synthesis to sintering. The case of alumina-based materials, Verres Céramiques and Composites 1/1 (2011) 62-75.

[9] G.A. Helvey, Finishing Zirconia Chairside. What dental technicians need to tell their dentist clients about the effects of surface grinding, Inside Dental Technology 2/2 (2011) www.dentalaegis.com/idt/2011/02/finishing-zirconia-chairside.

[10] J.F. Bartolome, A.H. De Aza, A. Martın, J.Y. Pastor, J. Llorca, R. Torrecillas, G. Bruno, Alumina/zirconia micro/nanocomposites: a new material for biomedical applications with superior sliding wear resistance, Journal of the American Ceramic Society 90/10 (2007) 3177-3184.

[11] R.P. Rana, S.K. Pratihar, S. Bhattacharyya, Effect of powder treatment on the crystallization behaviour and phase evolution of Al_2O_3-high ZrO_2 nanocomposites, Journal of Materials Science 41/21 (2005) 7025-7032.

[12] J.A. Tichy, D.M. Meyer, Review of solid mechanics in tribology, International Journal of Solids and Structures 37/1-2 (2000) 391-400.

[13] J. Prakash, D. Kumar, K. Mohanta, Mechanical behaviour of alumina-zirconia composites slurry method, International Journal of Engineering Science and Technology 3/2 (2011) 1359-1367.

[14] R.P. Rana, S.K Pratihar, S. Bhattacharyya, Powder processing and densification behaviour of alumina-high zirconia nano-composites using chloride precursors, Journal of Materials Processing Technology 19/1-3 (2007) 350-357.

[15] F. Kern, Microstructure and mechanical properties of hot-pressed alumina – 5 vol% zirconia nanocomposites, Journal of Ceramic Science and Technology 2/1 (2010) 69-74.

[16] U. Anselmi-Tumburini, J.E. Garay, Z.A. Munir, Fast low-temperature consolidation of bulk nanometricceramic materials, Scripta Materialia 54 (2006) 823-828.

[17] T. Fett, D. Munz, Subcritical crack growth of macrocracks in alumina with R-curve behavior, Journal of the American Ceramic Society 75/4 (1992) 958-963.

[18] M. Szutkowska, M. Boniecki, Crack growth resistance of Al_2O_3-$ZrO_{2(nano)}$ (12 mol% CeO_2) ceramics, Journal of Achievements in Materials and Manufacturing Engineering 22/1 (2007) 41-44.

[19] T. Fett, An analysis of the three-point bending bar by use of the weight function method, Engineering Fracture Mechanics 40/3 (1991) 683-686.